Multi-Scale Imaging of Corrosion and Hydrogen Embrittlement in Irradiated Nuclear Materials

David Simonne[1], Riley Hultquist[1], Sayantan Mondal[1], Anthony Guttiérez[1], Andrea Resta[2], Marilyn Sarkis[4], Jiangtao Zhao [4], Ericmoore Jossou[1]

[1]Massachusetts Institute of Technology - USA, [2]Synchrotron SOLEIL - France, [3]The European Synchrotron - France

Environments in nuclear systems

Ten percent of the world electricity is produced *via* nuclear reactors, in which structural components are exposed to an aggressive and complex environment over decades.

- Neutron radiation leads to atomic displacement / defects / dislocations.
- High temperature ($\approx 350\,°C$) and high coolant pressure (MPa).
- Mechanical stress, vibrations.
- Corrosive aqueous environment, radiolysis product / nuclear reactivity controlled with additives.
- Effects can take between minutes and years to manifest.

Radiation damage, corrosion and embrittlement

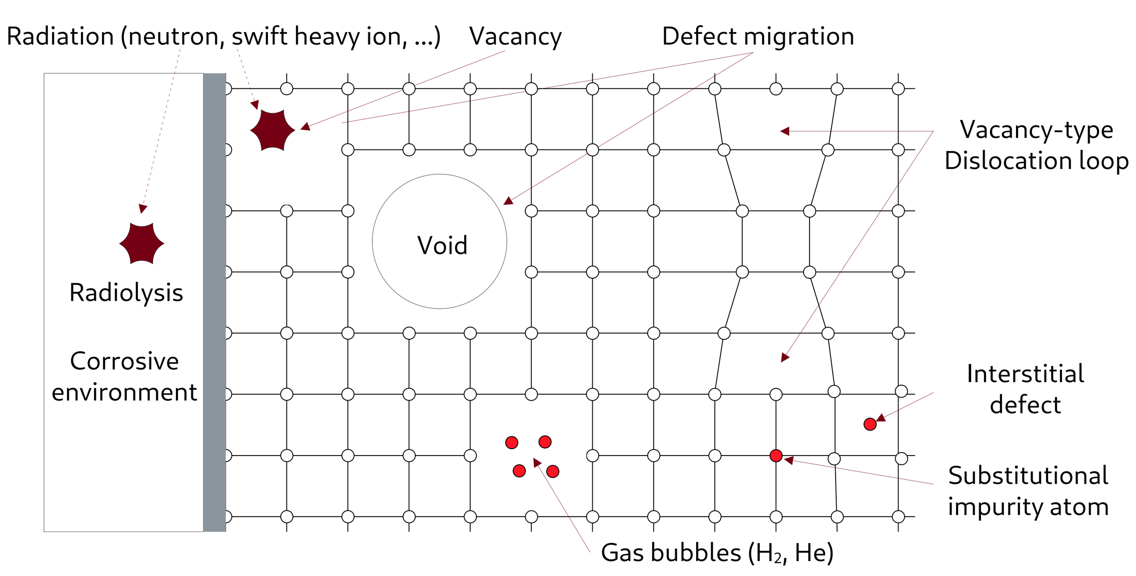

Figure 1. Neutrons can displace atoms, creating a variety of defects.

Which materials are present?

Large variety of alloys.

- Pressure vessel: ferritic steel.
- Corrosion resistant passivating layer: Ni-based alloys, Ni-Fe-Cr alloys, stainless steels.
- Fuel cladding: zirconia alloys.

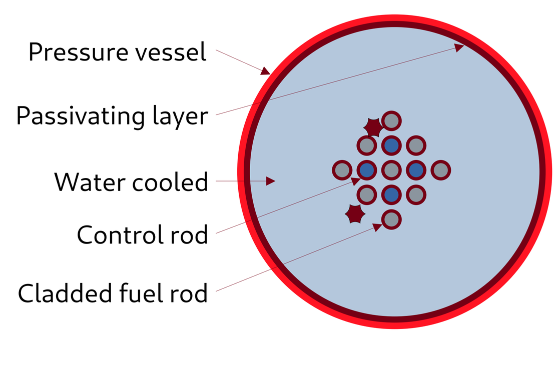

Figure 2. Light water reactor schematic.

Defect control

Heavy ion irradiation can reproduce neutron irradiation effects.

- Before / after irradiation.
- Ion of different nature -> interstitial defects.
- Ion nature, fluence and energy $\rightarrow$damage depth profile.
- We have a nuclear reactor & an ion accelerator.

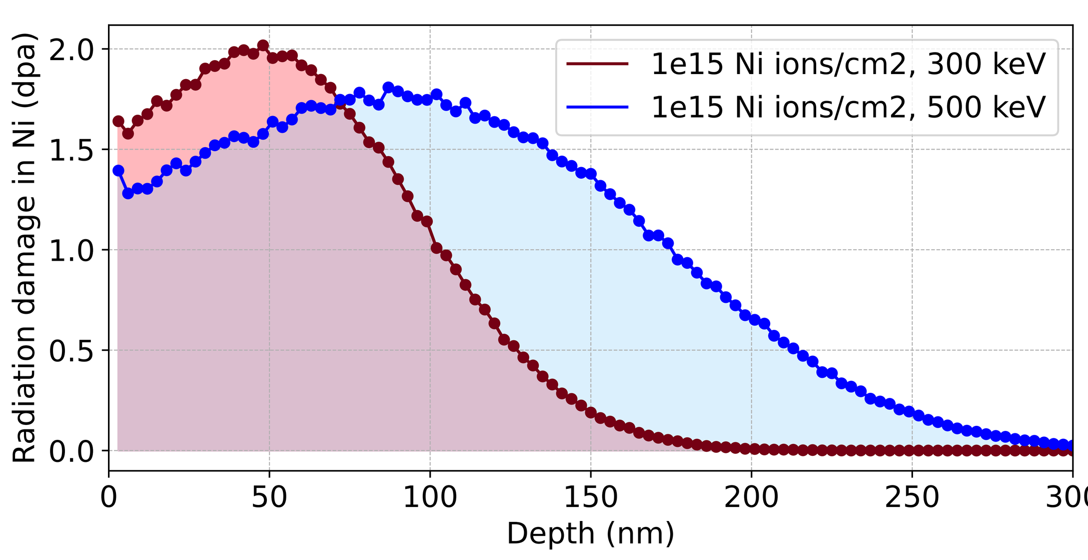

Figure 3. Ni ion radiation damage profile, computed with SRIM.

Nano-indentation allows dislocation studies.

- Before / after dislocation introduction.
- Dislocation type, role and mobility characterisation.

Synchrotron radiation for *operando* studies

1. How does neutron radiation affect structural materials?
2. How to measure the material's structural evolution in a **relevant** coupled environment?

Standard imaging techniques do not yet offer a combined access to **operando** and **high resolution** setups.

Synchrotron radiation provides intense, coherent, focused, and tunable X-rays that allow us to work in complex environments!

Measuring strain in three dimensions

Bragg Coherent Diffraction Imaging relies on:

- Highly coherent synchrotron sources.
- Samples below coherent volume: $\approx 1\,\mu$m^3.
- Highly faceted samples.

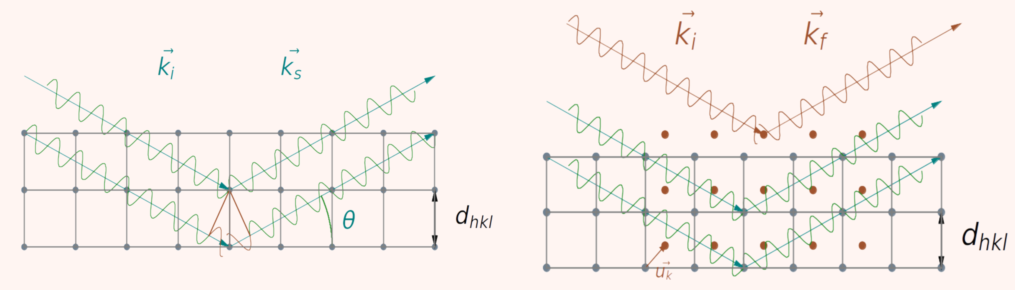

Access to **full displacement field** $\rightarrow$Defect identification!

Sample preparation

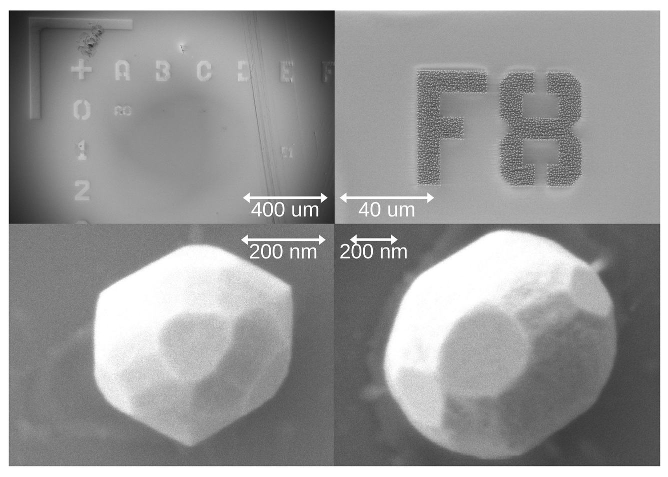

Figure 4. EBL pattern and Ni particles imaged by scanning electron microscopy.

1. Pattern drawn by electron beam lithography (EBL).
2. Crystallization by annealing in forming atmosphere.
3. SEM imaging and EBSD crystal orientation determination.

Sample characterisation

The interface plays a crucial role in the supported crystals shape, orientation, and strain field.

Substrate	Nb:SrTiO3(001)	SiO2(001)(1 ML) /Si(001)	SiO2(001)(2 ML) /Si(001)	SiO2(001)(3ML) /Si(001)	SiO2(001)	Si(001)
W_{sep} (J/m^2)	0.19	0.61	0.70	1.60	2.16	3.16
γ_{int} (J/m^2)	2.76	–	–	–	2.92	0.97

Table 1. Work of separation W_{sep} and interfacial energies (γ_{int}) for Ni(111) on different substrates.

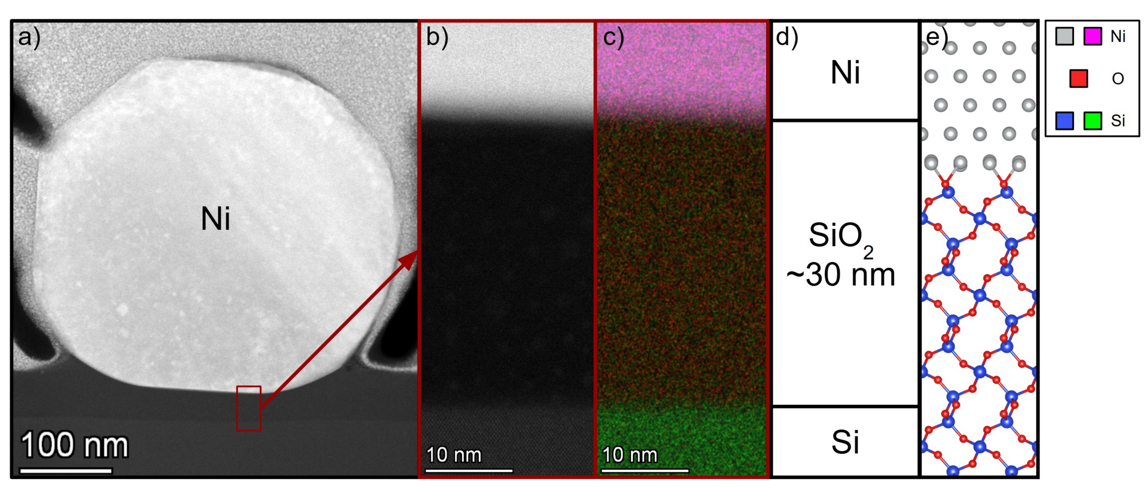

Figure 5. a) Cross-sectional TEM image of a Ni particle on SiO_2 / Si(001) substrate. b) Zoom on interphase boundary with c) EDS measurement and d) Interface schematic. e) DFT cell used for interface calculations in Tab. 1.

In situ electrochemical cell

The cell design must be compatible with each synchrotron beamline's unique setup.

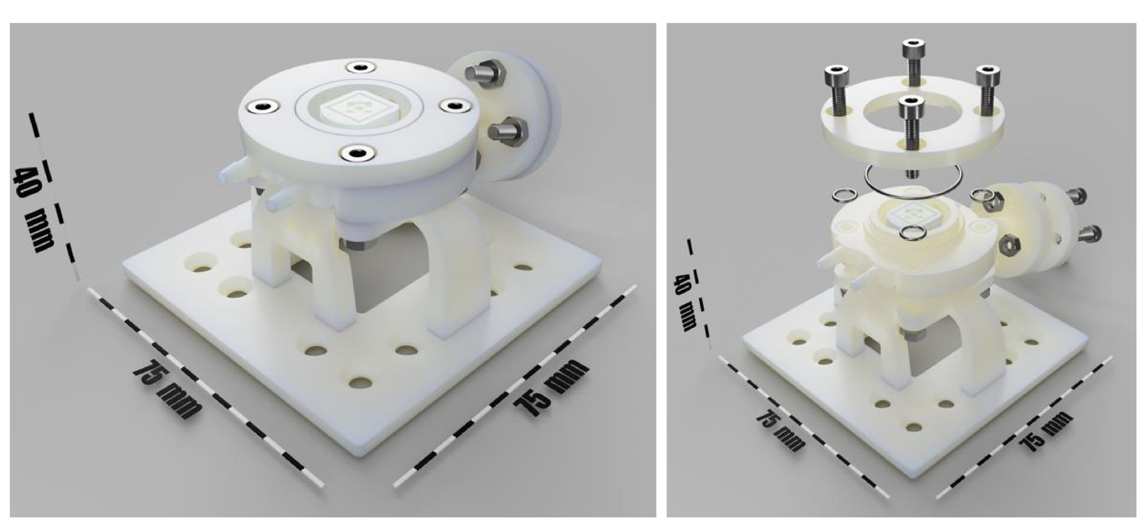

Figure 6. Electrochemical cell design, compatible with three electrode setup, liquid flow, and four different synchrotron beamlines.

- Can be used in the lab and at synchrotrons.
- Electrolyte flow.
- Accomodates working, counter and reference electrode.
- Easily shipped.
- Light for nano-positionning.
- 3D printed, easy to modify.
- Cheap.
- Modular design.
- Can be directly printed at synchrotrons.
- One cell / sample.
- One mount / beamline.

X-ray irradiation strain relaxation effect

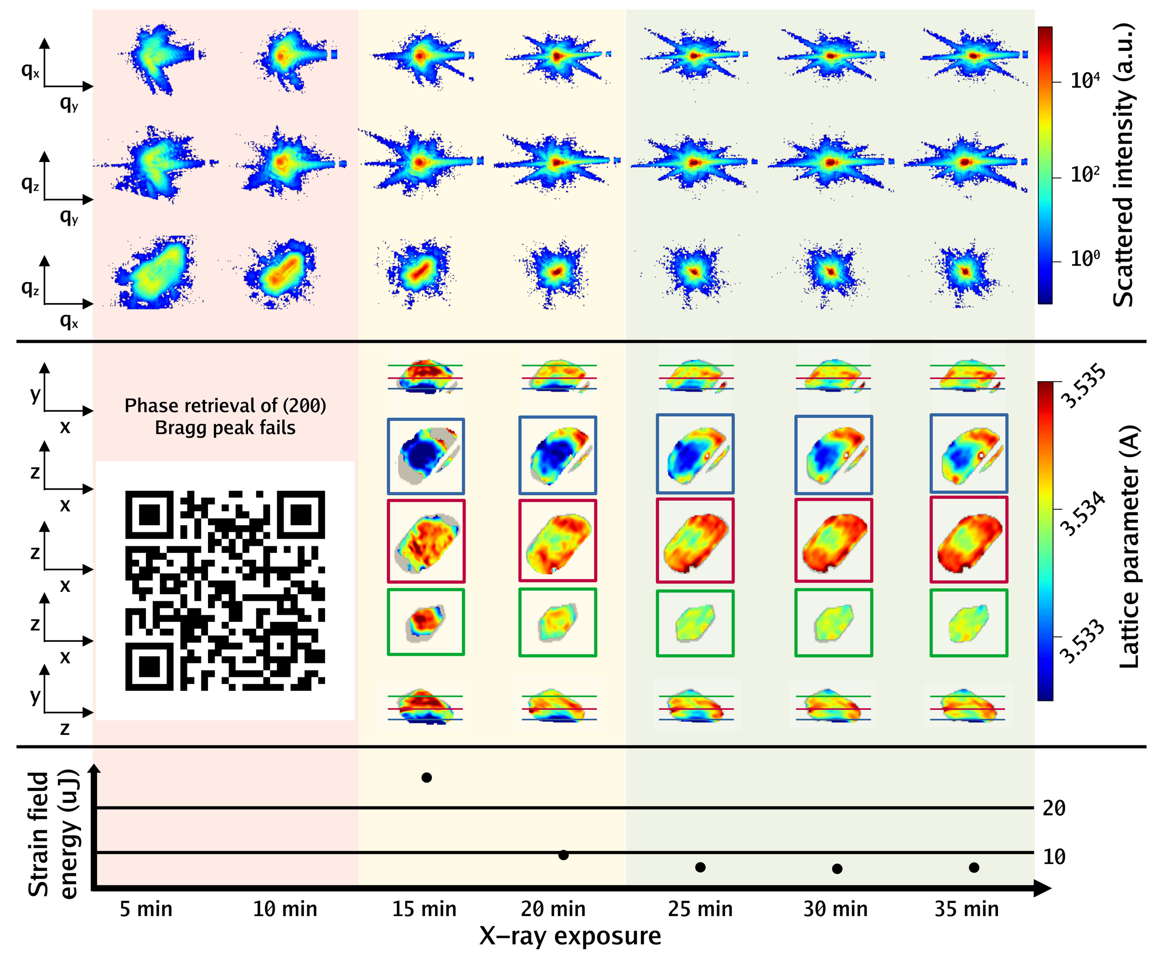

Figure 7. Strain relaxation of a Ni particle on SiO_2/Si(001) from highly fluent X-ray beam visible by Bragg peak assymetry (top) and strain field (middle). The strain field energy (bottom) presents a quantitative decrease of the strain field inside the particle.

Corrosion in light water reactor environment

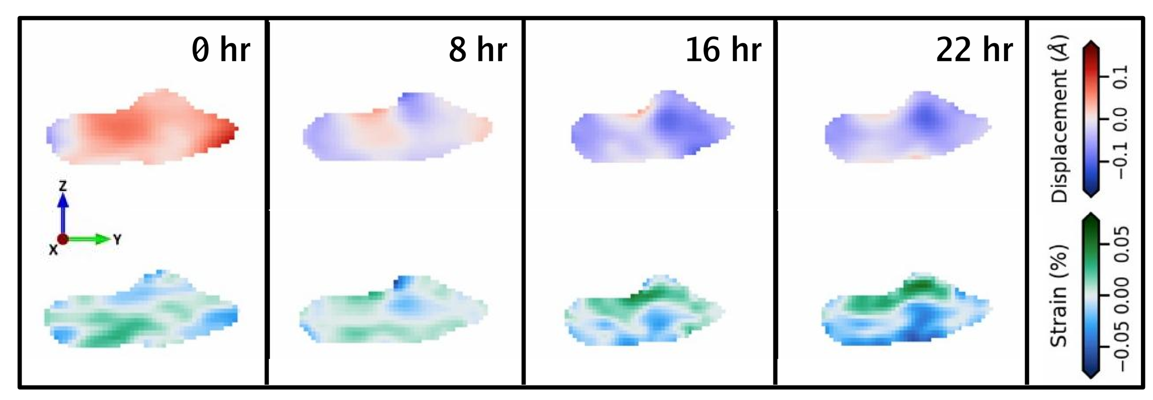

Figure 8. Strain buildup during corrosion of NiCo particle.

Defect signature in X-ray microscopy

Dark-field X-ray microscopy enables the visualisation of crystalline defects over extended ranges.

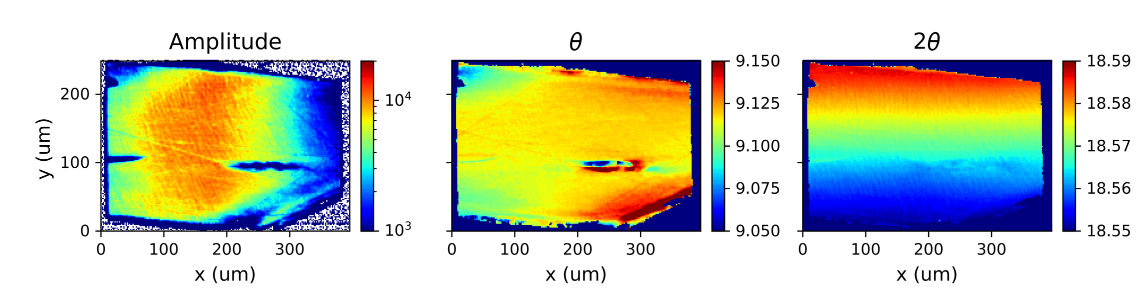

Figure 9. DFXM image of Fe single crystal. Dislocations are visible over several hundreds of micrometers before hydrogen embrittlement.

Key takeaways

- Synchrotron radiation allows *operando* studies.
- Strain signature is accessible *via* Bragg imaging techniques.
- Combining techniques allows nano as well as meso scale information.

Multi-scale approach, sensitive to material density, crystal structure, and defects, during *operando* studies.

References

[1] A. C. Bach, F. Martin, C. Duhamel, S. Perrin, F. Jomard, and J. Crepin. Hydrogen trapping by irradiation-induced defects in 316 lstainless steel: A combined experimental and modeling study. *Journal of Nuclear Materials*, 562:7–10, 2022.

[2] E. Jossou, T. A. Assefa, A. F. Suzana, L. Wu, C. Campbell, R. Harder, W. Cha, K. Kisslinger, C. Sun, J. Gan, L. Ecker, I. K. Robinson, and S. K. Gill. Three-dimensional strain imaging of irradiated chromium using multi-reflection bragg coherent diffraction. *npj Materials Degradation*, 6(1), dec 2022.

[3] F. Schmidt, P. Hosemann, R. O. Scarlat, D. K. Schreiber, J. R. Scully, and B. P. Uberuaga. Effects of radiation-induced defects on corrosion. *Annual Review of Materials Research*, 51:293–328, 2021.

[4] M. Short, D. Gaston, M. Jin, L. Shao, and F. Garner. Modeling injected interstitial effects on void swelling in self-ion irradiation experiments. *Journal of Nuclear Materials*, 471:200–207, 2016.

Acknowledgments

This work was funded by the Faculty Startup Fund support from MIT. The sample preparation work was carried out in part at MIT.nano, thanks to the help of Dr. Aubrey Penn and Juan Fererra. We acknowledge the ESRF and SOLEIL synchrotrons in France for providing beamtime utilizing beamline ID01 and SixS. We used the HPC at INL, supported by the Office of Nuclear Energy of the U.S. DOE and the NSUF under Contract No. DE-AC07-05ID14517.

Nuclear Science and Engineering